IOP Publishing Journal Title
Phys. Med. Biol. **XX** (XXXX) XXXXXX https://doi.org/XXXX/XXXX

A Static Beam Delivery Device for Fast Scanning Proton Arc-Therapy

K P Nesteruk[1], A Bolsi[1], A J Lomax[1,2], D Meer[1], S van de Water[1] and J M Schippers[1]

[1] Paul Scherrer Institute, Villigen PSI, Switzerland
[2] Department of Physics, ETH Zurich, Switzerland

E-mail: konrad.nesteruk@gmail.com and marco.schippers@psi.ch

Keywords: proton-arc therapy, static beam delivery device, fast dose delivery

Abstract

Arc-therapy is a dose delivery technique regularly applied in photon radiation therapy, and is currently subject of great interest for proton therapy as well. In this technique, proton beams are aimed at a tumor from different continuous ranges of incident directions (so called “arcs”). This technique can potentially yield a better dose conformity around the tumor and a very low dose in the surrounding healthy tissue. Currently, proton-arc therapy is performed by rotating a proton gantry around the patient, adapting the normally used dose-delivery method to the arc-specific motion of the gantry.

Here we present first results from a feasibility study of the conceptual design of a new static fast beam delivery device/system for proton-arc therapy, which could be used instead of a gantry. In this novel concept, the incident angle of proton beams can be set rapidly by only changing field strengths of small magnets. This device eliminates the motion of the heavy gantry and related hardware. Therefore, a reduction of the total treatment time is expected.

In the feasibility study presented here, we concentrate on the concept of the beam transport. Based on several simple, but realistic assumptions and approximations, proton tracking calculations were performed in a 3D magnetic field map, to calculate the beam transport in this device and to investigate and address several beam-optics challenges. We propose and simulate corresponding solutions and discuss their outcomes. To enable the implementation of some usually applied techniques in proton therapy, such as pencil beam scanning, energy modulation and beam shaping, we present and discuss our proposals.

Here we present the concept of a new idea to perform fast proton arc-scanning and we report on first results of a feasibility study. Based on these results, we propose several options and next steps in the design.

1. Introduction

1.1 Arc therapy

In radiation therapy with beams of high energy X-rays (photons) or protons, the dose is usually applied by irradiating the tumor from several directions, in order to limit the dose in healthy tissue in vicinity of the tumor. To irradiate the tumor from different directions, the beam delivery device (i.e. the gantry) rotates around the patient to get several irradiation directions (see figure 1a). In devices recently developed for X-ray therapy (Accuray 2020, Teoch *et al* 2011), this is exploited maximally by so-called arc-irradiations. In this technique the irradiation device is rotating along one or more arcs around the patient, while continuously administering the dose (see figure 1b). Alternative arc delivery techniques, such as volumetric-modulated arc therapy, which delivers intensity modulated-like dose distributions in 1-2 rotations, have been developped by other vendors (Chiavassa *et al* 2019). For both delivery paradigms, the dose rate, rotation speed and field shape vary synchronously with treatment angle. With this technique a larger volume of healthy tissue receives dose, but in general at a lower dose level than in techniques using a limited number of fields. More importantly, rotational treatments with photons have had a significant

impact on treatment efficiency. These clear gains in conventional therapy have motivated several groups and industry to apply this technique in proton therapy as well. In 1997 *Proton Arc-therapy* has been proposed (Sandison G A *et al* 1997), in which the advantages of the dose distribution in proton therapy are combined with the irradiation of a tumor from a large and continuous range of angular directions.

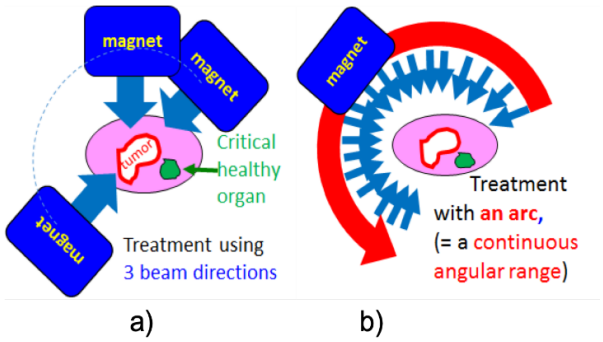

Figure 1. a) Schematic view of the cross-fire technique by rotating a gantry with magnets of the beam transport around the patient to a few discrete treatment angles. b) Radiation during a continuous change of the treatment angle yields an irradiation from a so called "arc". Of note, a number of arcs can be applied.

In Beaumont Cancer Center (Ernult 2018) proton arc-therapy is being applied by using a specially developed algorithm for optimum dose delivery, applying many discrete angles (Ding *et al* 2016). However, for proton therapy there are major technical limitations with gantries when applying arc therapy. The large dimensions (8-12 m diameter) and masses (100-200 tons) of the proton gantries, e.g. (Schulze 1991), limit the rotational speed to 1 turn/minute for safety measures preventing possible collisions, a speed that is in the same order of magnitude as the 1 turn/75 sec in the RapidArc Photon treatment system of Varian (Nicolini 2011). In proton therapy the gantry has to rotate the beam delivery equipment in the nozzle and the large magnets in the final part of the beam transport system around the patient with a beam positioning accuracy better than a millimeter. This is motivating interesting studies to optimize the treatment plan to obtain a maximal benefit in the existing clinical sytems (Ding X *et al* 2016). For example, in the work presented by Li et al (Li *et al* 2019), it is shown that a proton-arc treatment of a partial brain case could be done in about 4-5 minutes.

1.2 Goal and concept of the new Proton Arc-Scanning device

Here we report on a feasibility study of a conceptual design of a static beam delivery device, in which no heavy magnets are needed to move while applying fast arc therapy with a proton beam, as presented in figure 2.

The device consists of a cylindrical field free region for the patient, surrounded by two concentric cylindrical regions with axially oriented magnetic fields. The beam from the accelerator is entering the device from the side in a tangential direction. For the calculations done in our design studies, we have used an incoming vertical beam direction at the lower right side, but any other position can be chosen as well. The conceptual idea of its operation is illustrated in figure 3.

The *Guiding field* in the outer cylindrical region is a static magnetic field, guiding the incoming beam along a circular track around the patient. At a certain point the beam will enter the enclosed *Bending field* region, in which a stronger static magnetic field will bend the beam into the direction of the isocenter (the location where all beams cross) on the cylinder axis. The patient is located at a treatment table in the *Central region* in the core of the device. At the patient the treatment angle is determined by the azimuthal location where the beam has entered the *Bending field* region. This location is set by the strengths of so-called *Arc-Scanning Magnets (ASMs)* only. The ASMs are located at the point where the beam enters the outer ring of the device.

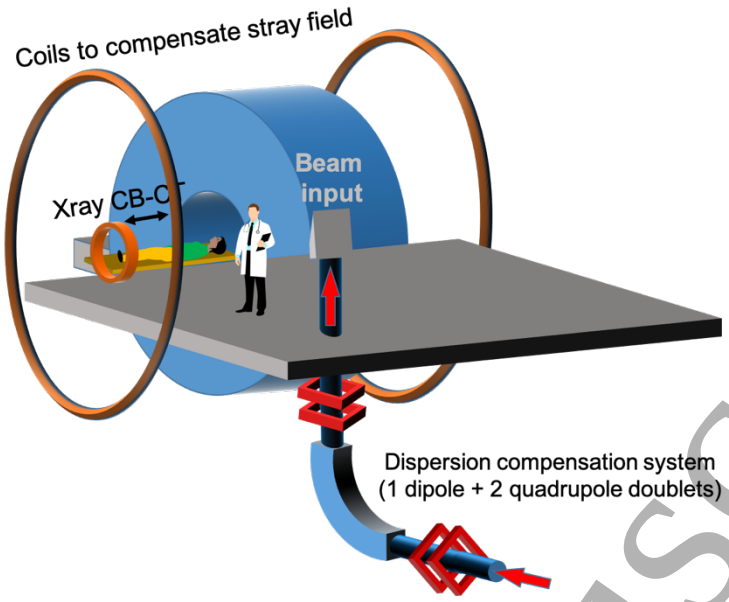

Figure 2. Schematic view of the static fast proton-arc therapy system[1], in a treatment room. The treatment table with the patient slides through the device. In the configuration shown here, the beam from the accelerator is coming from below and brings the beam into the arc-scanning device on the right-hand side.

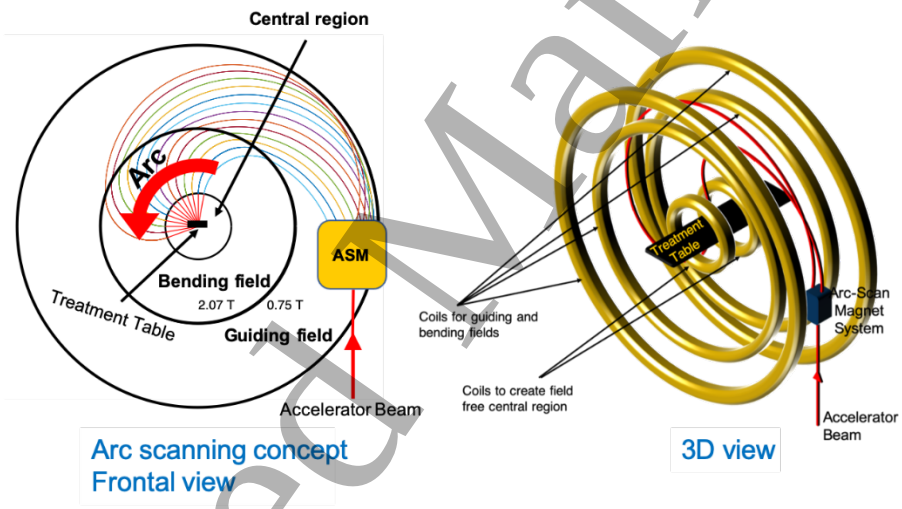

Figure 3. Schematic view of the principle of operation of the static beam proton-arc therapy device. The device consists of three major concentric regions, consisting of the *Guiding field*, in which the beam is sent to the appropriate azimuthal angle, the *Bending field*, in which the beam is aimed at the tumor, and the *Central region*, in which the patient is located at the treatment table. A possible arc of beams creating a continuous range of treatment angles is indicated. These treatment angles are set by only adjusting the Arc-Scan Magnet system (ASM).

1.3 Methods of beam delivery in the proton-arc therapy device

In this concept of an arc-scanning device, the beam is not rotated by a gantry rotation, but only by adjusting the strengths of a set of small steering magnets, the ASMs. These adjustments of the ASMs will be small, so that these can rapidly cover a

[1] Patent has been granted under No. 19702021.7 – 1122

substantial arc span within a fraction of a second. This is obviously superior to the much slower gantry rotation and, as we will discuss later, it opens possibilities of further optimizing the beam delivery process.

The arc-scanning will be extended by pencil beam scanning (PBS), to cover typical target volumes. In this study we have investigated PBS within the bending plane. We will show that scanning can be performed by slight adjustments of the ASMs. For PBS in the axial dimension, the ASMs have to deflect out of the bending plane, in combination with shifting the patient table along the axis. This can be done in steps (irradiated parallel slices) or continuously, so that the dose is delivered along a helix, in analogy to the Tomotherapy device (Accuray 2020), used in photon treatments. The design presented here, will offer proton-arc treatments, together with an extremely rapid 2D dose application within an arc.

2. Materials and Methods

Our feasibility study has concentrated on beam transport and associated magnetic field specifications. In this section some essential parameters will be defined and different techniques used in this study will be described.

2.1 Magnetic field map

The combination of a non-conventional beam transport and the special magnetic field configurations has shown to be a critical challenge. Here we describe the methods used to calculate magnetic field and perform particle tracking.

Initial tracking calculations have been performed in a model made in Matlab (Matlab 2020), which is based on a very simple configuration of two concentric regions of homogeneous magnetic fields, surrounding the field free *Central region*. With these calculations we have tested the concept and identified potential problems in the beam transport in this new operation principle. Variables used in our study are defined in figure 4.

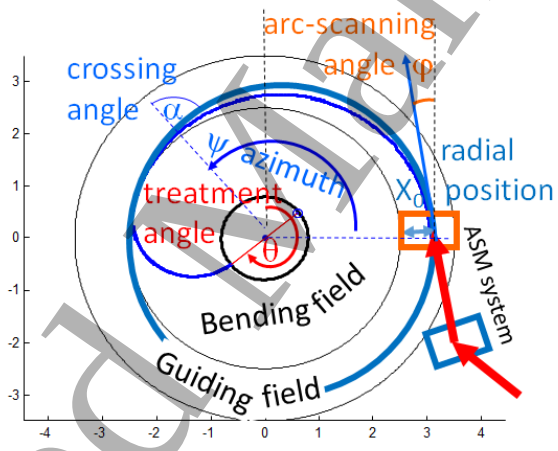

Figure 4. Definition of the variables used in this study. The orbit in the *Guiding field* starts at the ASM system in direction φ at radial position x_0. At azimuthal angle ψ this circular orbit crosses the border with the *Bending field* at crossing angle α. In the *Central region* the beam is aimed to the isocenter at treatment angle θ.

In a next phase more realistic simulations have been performed by 3D particle tracking in Magnetic fields, which have been calculated using extrapolations from a very simple magnet model (see figure 5). Using POISSON SUPERFISH (Menzel and Stokes 1987) and ZGOUBI (Meot 2012), a 3D map of the magnetic field has been generated. This method ensured us to obtain realistically shaped magnetic fields that obey Maxwell's equations.

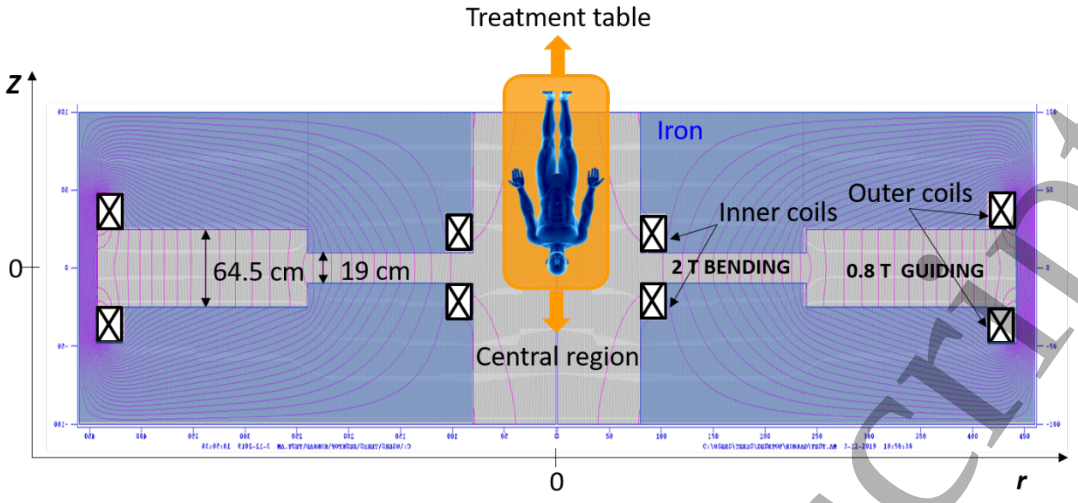

Figure 5. Top view of a horizontal cross section through the magnet. The patient table is located in *Central region*. It is surrounded by the magnet, consisting of an iron yoke and two pairs of coils. This encloses the *Guiding field* region, in which the protons are guided to the appropriate entrance into the 2 T *Bending field*. This *Bending field* will bend the protons towards the tumor.

As shown in figure 5, the simple magnetic model of the system consists of two pairs of coils, iron and air gaps. Outer coils with a current of 250 kA create both the *Guiding field* and the *Bending field* with the help of a properly shaped iron pole. The -150 kA negative current in the inner coils makes the *Central region* field free.

POISSON was used to calculate the 2D magnetic field in the R-Z plane, assuming axial symmetry around the common Z-axis of the cylinders. The different field strengths of the *Guiding field* and the *Bending field* have been achieved by selecting different pole gaps in the different regions. Since the only goal of these calculations was to achieve realistically shaped magnetic fields, no effort has been made to minimize the amount of iron, or to optimize the coil. Figure 6 shows the resulting magnetic field profile B_z as a function of radius in the midplane.

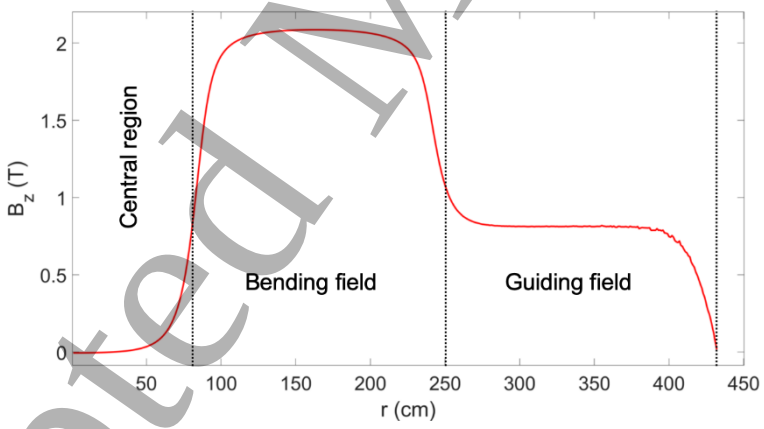

Figure 6. Magnetic field profile in the midplane calculated in Poisson Superfish.

This axially symmetric field was extrapolated to obtain a 3D field. However, we did not simply rotate this field around the symmetry axis, since the iron pole would give limitations in the axial direction. These might intercept particle tracks. Also, the field shape is defined very strictly by the shape of the iron, when approaching the poles. This limits the needed extension of the field maps into the axial direction. Therefore, we have chosen to perform the extrapolation in two steps, with the 1D radial field profile in the axial midplane of the magnet as our starting point. In the first step we used the cylindrical symmetry to create a 2D field map in the X-Y mid plane by rotating the field along the Z-axis around the symmetry axis. In the second step this midplane field has then been extrapolated into the axial direction using the code ZGOUBI. This code uses a special procedure, which allows magnetic fields to be extrapolated based on Maxwell's equations by Taylor expansion up to fourth order.

2.2 Beam transport

These realistically shaped magnetic fields, with grid step sizes of (r, θ, z)=(1 cm, 157 mrad, 1 cm) have been used to perform particle tracking calculations. These were performed using the codes OPAL (Adelmann *et al* (2008–2018)) and COSY-Infinity (Berz 1990). From the tracking calculations with OPAL we selected reference trajectories, starting at the second magnet in the ASM system. At that starting point we assumed the usual beam sizes of cyclotron beams entering a gantry and we have investigated if typically used pencil beam sizes can be achieved at the isocenter. The radial starting positions and directions of the reference trajectories depend on the treatment angle and were derived from the Matlab calculations. In locations of complex field shapes we have performed multiple particle tracking in the 3D field map, with a step size of 0.01 ns in OPAL. To optimize several beam transport details in regions where the field could be described by a multipole expansion, COSY-Infinity has been used. In COSY the beam optics was described as the transport through a series of consecutive magnetic multipoles. We derived the parameters describing these multipole fields from the magnetic fields crossed by the reference trajectory in the 3D field map. Our beam transport study has concentrated on beam direction issues and minimization of the beam spot size at the isocenter. In the section Results and Analysis we will report on an investigation of the following beam transport issues:

- Demonstration of the validity of the concept
- Overfocusing of the beam, when crossing the boundary between *Guiding* and *Bending field*
- Defocusing of the beam in the *Guiding field*
- Pencil beam scanning, energy variations

After these beam transport issues, we will also discuss beam monitoring and beam handling and the possibility to perform non-coplanar irradiations in the proposed proton arc-scanning device.

3. Results and Analysis

3.1 Test of operation principle

In a Matlab model, the parameters describing the three different regions, were defined as given in table 1.

Table 1. Dimensions and field strengths in the different regions, as used in the initial Matlab calculations.

Region	**covered radial range (m)**	**magnetic field strength (T)**
Inner region	0 … 0.8	0
Bending field	0.8 … 2.5	2
Guiding field	2.5 … 3.4	0.8

The fields in the *Bending field* region and in the *Guiding field* region were assumed to be homogeneous. Unless mentioned otherwise, all calculations have been performed with 230 MeV protons, the maximum energy typically used in proton therapy. In the *Guiding field*, these will describe a circle with a radius of 2.9 m. The ASMs set the starting radial position x_0 and direction φ of the beam. These starting-point parameters have been derived from a circle that touches the boundary between the *Guiding* and *Bending field*, as shown in figure 4. This touching point is where the beam enters the *Bending field*. The azimuthal position ψ of this touching point determines the treatment angle θ. In this concept-test we used the ASM to set the azimuthal angle ψ. As will be shown later, also smaller circles crossing this field boundary could be chosen to have a less shallow touching angle α, so that the circles intercept more clearly. But to start with, we used this touching-circle concept.

At the location ψ, where the trajectory enters the stronger *Bending field*, it is bent to the patient along a circular trajectory with a radius of curvature of 1.16 m. It is important to note, that we have decided for a design in which the angle at which the boundary field is crossed, is the same for all the azimuthal angular positions of the crossings. This means, that the track shape in the *Bending field* region is independent of the length of the trajectory in the *Guiding field*. This symmetry is a very important characteristic of the device and, as will be discussed later, the *Guiding field* has to be designed such that this requirement is met. The strength of the *Bending field* is such, that the trajectory will cross the boundary to the central field free region perpendicularly, so that the straight track in this central region goes along the radial direction towards the central axis.

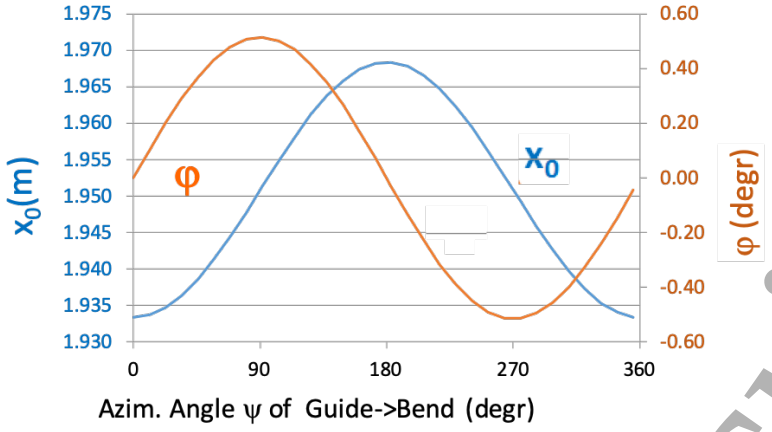

Figure 7. The starting conditions x_0 and φ of the "touching circle" trajectory in the second magnet in the ASM, as a function of the azimuthal position ψ, where the beam "touches" and enters the *Bending field* region.

The second magnet in the ASM is used as the starting point of the beam tracking. The radial position x_0 in this ASM magnet is determined by the deflection of the first magnet in the ASM and the beam direction φ is determined by the deflection of the both ASM magnets. Figure 7 shows these values as a function of the azimuthal angle ψ, where the trajectory enters the *Bending field*. It shows that the needed ASM deflections for 230 MeV protons cover a small range and do not require very special magnets. Therefore, when taking care about shielding of the main field, the ASM system is not expected to be a technical problem.

A very accurate calibration of the ASM system is needed. Special care must be taken at sensitive ranges of the ASM magnetic fields, at which a minor change of an ASM would yield a big shift in azimuthal angle. These occur at the maxima and minima of the curves shown in figure 7, where the derivatives are minimal. We have investigated this sensitivity in a model with two ASM sets, as shown in figure 8a. At all treatment angles we found that an error in starting angle φ of approximately 0.3° will cause an error of 1° in treatment angle θ. For the sensitivity of θ to x_0, we found that a 1^0 error is caused by a 5 mm error in x_0. These sensitivities are not expected to be a problem and relatively easy to deal with in accurate ASM systems. In general, when several ASM sets are mounted in the device, the sensitivity to the starting conditions could be reduced due to the shorter distances to be covered.

From these Matlab calculations of the reference trajectories, we concluded that the operational concept of the arc-scanning device is realistic. In the following subsections, we will discuss several detailed calculations and show how further optimizations can be achieved.

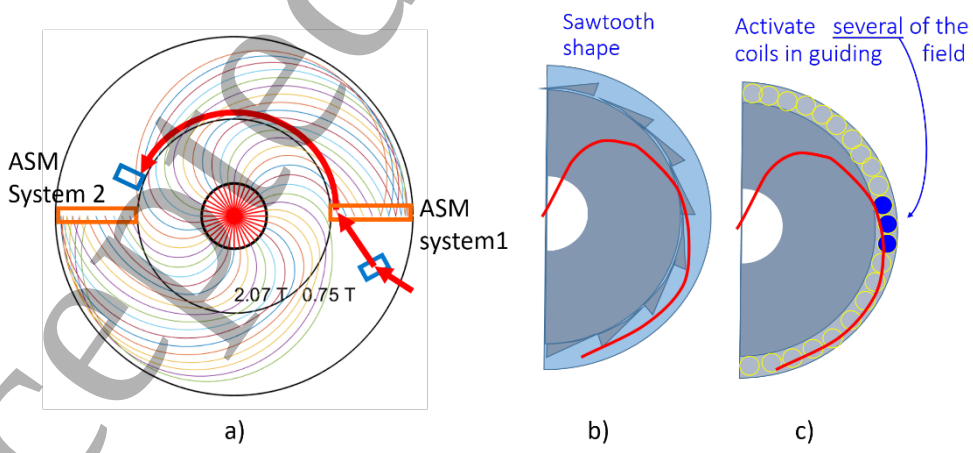

Figure 8. a) shows the concept of two ASM systems, each covering 180 degrees. The second ASM is reached by a special setting of the first ASM, at the beam entry point. b) and c) show configurations in which the boundary between the *Guiding field* and the *Bending field* is crossed less oblique, by adding a sawtooth-shaped pole edge or a series of coils in the *Guiding field* respectively.

In order to obtain a reasonable beam size at the isocenter, focusing of the proton beam has to be optimized. Special attention has been given to the very oblique, almost parallel crossing of the magnetic field boundary between the *Guiding field* and the *Bending field*, as we have in figure 4. This will cause a strong over-focusing, so effectively a large increase of the beam size in the non-bending plane, i.e. in the axial direction.

The most straightforward method to minimize this effect is to change the orientation of this field boundary, as encountered by the beam. In this first group of solutions shown in figure 8 b and c, the boundary crossing is made more perpendicular. This can be done by giving the outer edge of the *Bending field* a saw-tooth like shape (figure 8b). However, these triangular shaped "teeth" must have a minimum dimension of at least the pole-gap, to achieve the desired change of the field boundary shape. This would discretize the arc, so that continuous arcs are not possible anymore. A more continuous solution could be made by adding a series of small coils to the *Guiding field* region, as indicated schematically in figure 8c. Excitation of only the few coils near the boundary crossing point, will start the bending at an earlier moment. Disadvantages of this method are the large number of coils (i.e. costs) and the possible reduction of the arc-scanning speed, due a limited ramping speed of these coils.

Another solution uses a modification of the magnetic field strength's radial profile at the field boundary. This option has been studied in more detail in two steps. First, we have increased both the *Guiding field* strength and the radial width of the *Guiding field* region. In the *Guiding field* the trajectories thus followed a circular track with a smaller radius than the "touching circle" shown in figure 4. The combination of a smaller bending radius and approaching from a larger distance from the *Bending field* boundary enables a smaller α, so less obliquely. As shown in figure 9a, such tracks need more space, which is obtained by an increase of the radial dimensions of the device. However, already when the angle α is only a few degrees less than the catastrophic 90^0, a strong decrease of the over-focusing is achieved. In our model we have chosen $\alpha=70^0$, which needed an increase of the radius of the *Guiding field* region to 4.4 m and required an additional ASM in order to cover all the treatment angles (360^0). Figures 10 a, b and c show results of the tracking calculations from the ASM to the isocenter with OPAL. At the ASM we started with an RMS beam emittance of 2.25 mm x 0.5 mrad in both the bending and the non-bending planes. The catastrophic over-focusing did not occur at this crossing angle $\alpha=70^0$ and in the bending plane a very small beam size is obtained at isocenter. However, the obtained RMS isocenter beam spot size of RMS=4.5 mm in the non-bending plane, would still be too large. Therefore, as a second step, we modified the radial profile of the magnetic field boundary. We added a field bump, followed by a field dip in the radial direction, as shown in figure 9b. When crossing the subsequently obtained field gradients, these will cause a respective focusing and defocusing of the beam. Such ripples in the field could be generated by adding iron and/or a special shape of the coil or an extra coil at this radius.

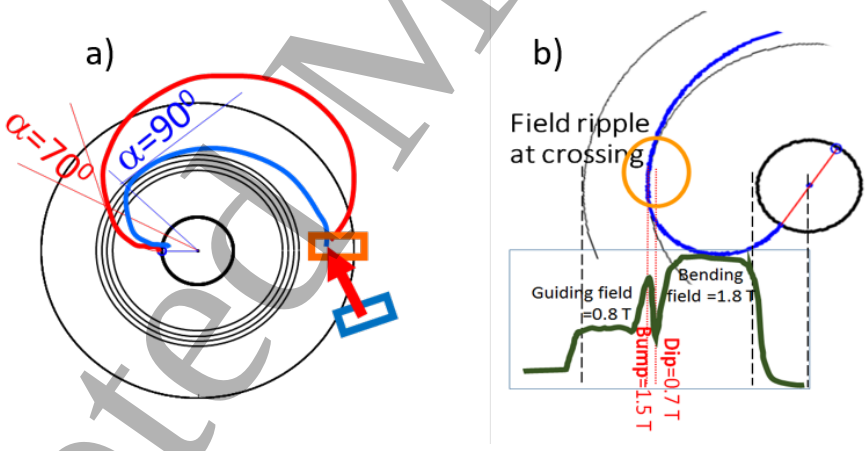

Figure 9. a) The field-boundary crossing angle α can be decreased by increasing the *Guiding field* strength and a larger device radius in addition. b) The ripple in the radial profile of the magnetic field at the boundary between *Guiding* and *Bending field*.

The required magnitudes of bump and dip have been estimated by COSY beam transport calculations through two bending magnets, with two short (more and less) bending magnets in between. In this configuration of a beam transport system without drift spaces between the magnets, we used pole faces inclined by 70^0 with respect to the beam direction at the inner magnet entrances and exits when simulating the crossing of the successive field strengths.

As explained in section 2.1, we used the code ZGOUBI to create a new 3D field map, which included the field bump and dip, to perform particle tracking from the ASM to isocenter. In this model we did not investigate in detail how this ripple in the field is realized, but modified the radial field profile by hand, using realistic radial field gradients. This modified radial profile

was then extrapolated as before. A practical realization can be made by, for example, additional concentric coils at this field boundary, or by modifying the pole edge, when using iron.

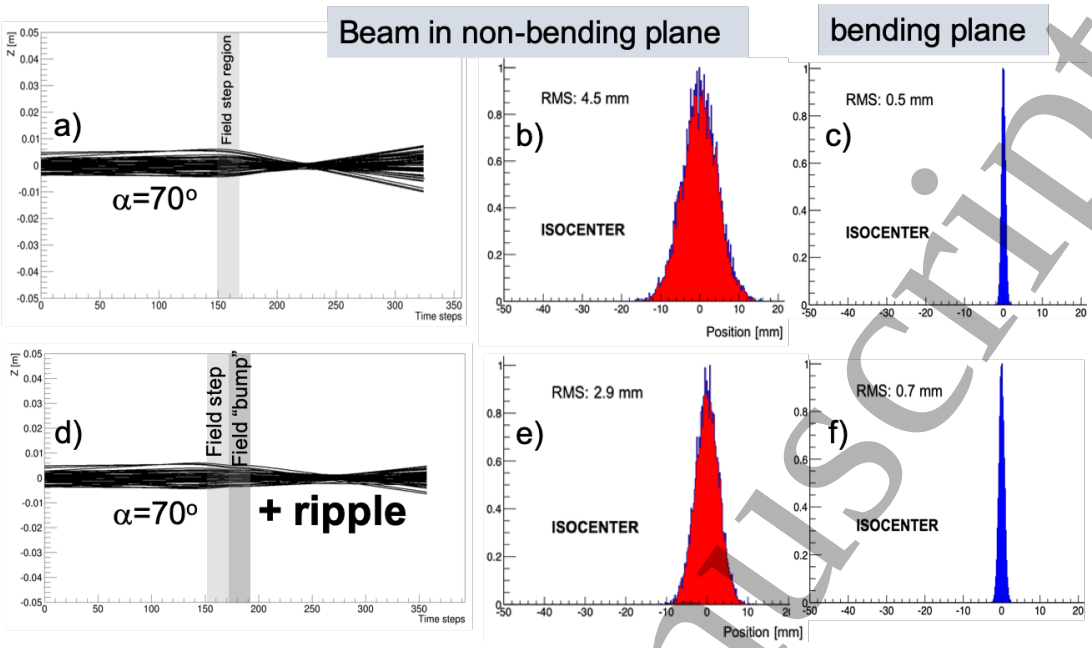

Figure 10. OPAL-Tracking results showing the beam in the non-bending (axial) plane and the beam profiles at the isocenter, for field boundary crossing without (a, b, c) and with (d, e, f) the ripple in the radial profile of the magnetic field.

As presented in figure 10 d, e and f, particle tracking in OPAL showed that this combination of a boundary crossing of $\alpha=70^0$ with the alternating focusing and defocusing in the "ripple", keeps the axial beam size at isocenter limited to 1.25 times the beam width in the arc-scanning magnet. The beam size in the bending plane direction increased slightly, but remained very small. Although many detailed calculations and eventual field modifications are still needed for further optimization of the boundary crossing, we observed that this method of a slight deviation from the almost parallel crossing in combination with a ripple in the radial field profile, offers enough flexibility to prevent a catastrophic over-focusing and to obtain appropriate beam sizes at isocenter. Of course, effects on beam size due to a vacuum window and monitors, have to be considered in a later phase of the design.

3.2 Focusing in the Guiding field

The beam transport in the homogeneous field shape of the *Guiding field* region, gives an automatic weak focusing of the beam in the bending plane. However, in the axial direction, perpendicular to the bending plane, there is no focusing at all. The length of the beam path in the *Guiding field* from the AMS to the crossing of the boundary with the *Bending field*, depends on the treatment angle. Therefore, apart from beam losses, the lack of focusing would also cause a beam size dependence of the treatment angle at the isocenter. We have implemented some focusing in the *Guiding field* by adding a periodic field modulation in the azimuthal direction. This is in analogy to the Thomas focusing based on hills and valleys in the poles of a cyclotron magnet, as described for example by Cradock (2009). In order to prevent a treatment angle dependence of the beam size at isocenter, we used a periodicity of 5^0. and a field modulation of 0.1 T in the 72 hills and valleys. This angular periodicity is of a similar magnitude as the step size used in discretized proton arc therapy (Ding *et al* 2016), where such a small periodic effect is acceptable.

The beam transport in the modulated *Guiding field* has been simulated in COSY. The beam path was described as a consecutive sequence of bending magnets with alternating field strengths of 0.7 and 0.8 T and boundaries with a few degrees pole face rotation in the bending plane. In our model there were no drift spaces between the bending magnets. Depending on whether the track is leaving the *Guiding field* within a hill or within a valley, the angle α at which the beam crosses the last boundaries of the modulation is a bit smaller or larger. Furthermore, the periodic focusing causes a small oscillation with a long periodicity in the beam envelopes in both planes. These are similar as the well-known betatron oscillations in accelerators. The effect of this dependence should be minimized, and therefore we have designed this betatron frequency (number of oscillation

periods along the circumference) to be approximately equal in both planes and not much larger than 1. By studying the possible combinations of the amplitude of the field modulation and pole face rotations, we found that the smallest dependence is obtained at a betatron frequency of approximately 1.4, a modulation amplitude of 0.1 T and a pole face rotation (edge tilt angle) of approximately 6 degrees. Figure 11 shows the results of the COSY calculations of the beam transport in the *Guiding field*, without (a,b,c) and with (d,e,f) the optimized field modulation.

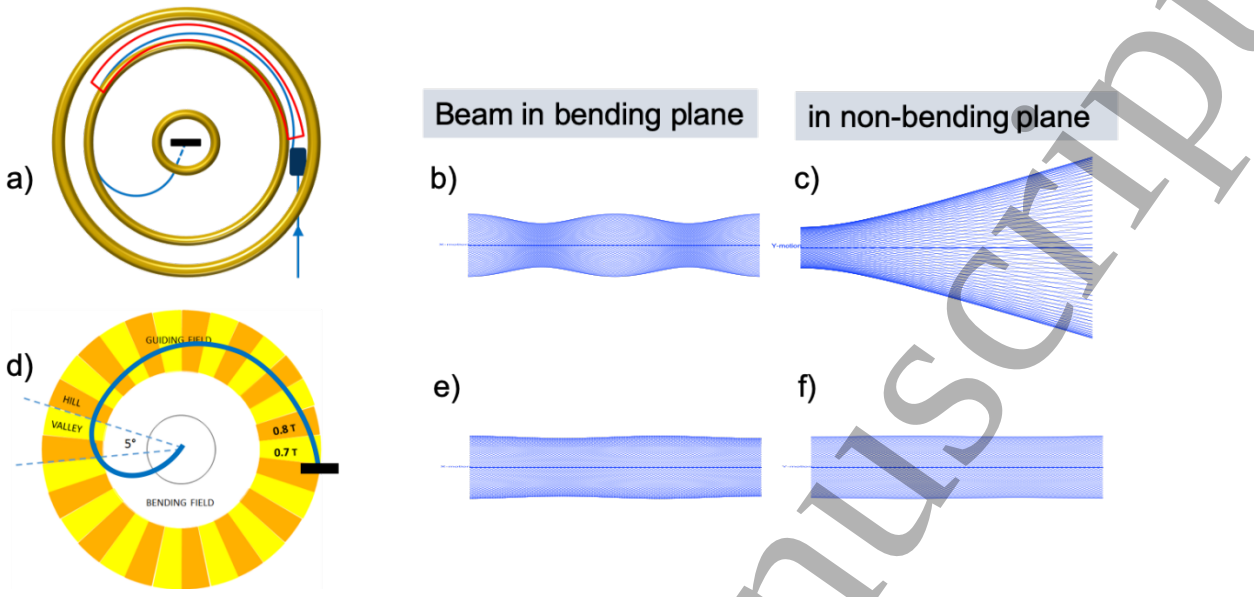

Figure 11. In a homogeneous *Guiding field* (a) the beam is focused in the bending plane (b), but not in the vertical non-bending plane (c). By varying the *Guiding field* azimuthally (d), focusing is achieved in both planes (e,f).

The COSY calculations show, that the field modulation keeps the beam size very constant in both planes. Therefore, the angle at which the beam crosses the boundary with the *Bending field* will not vary much, and the very small spot size dependence at isocenter as a function of azimuthal path length in the *Guiding field* (i.e. treatment angle θ) can be neglected.

3.3 Pencil beam scanning

To cover target volumes larger than several cubic centimeters, one could apply PBS in the arc-scanning device. The most trivial solution to implement such a system, would be to add dedicated scanning magnets in the field free central region or in the Bending-field region. However, since the necessary mechanical motions with treatment angle would compromise the arc-scan speed, one could consider a ring of coils, in analogy to the ones shown in figure 8c.

We investigated a PBS application based on the use of the ASM System. PBS was performed within the bending plane by adjusting the second magnet in the ASM. We found that an adjustment of the arc-scanning angle φ by ± 50 mrad, shifts the beam in lateral direction by ±4.2 cm at the isocenter, as shown in figure 12a and b.

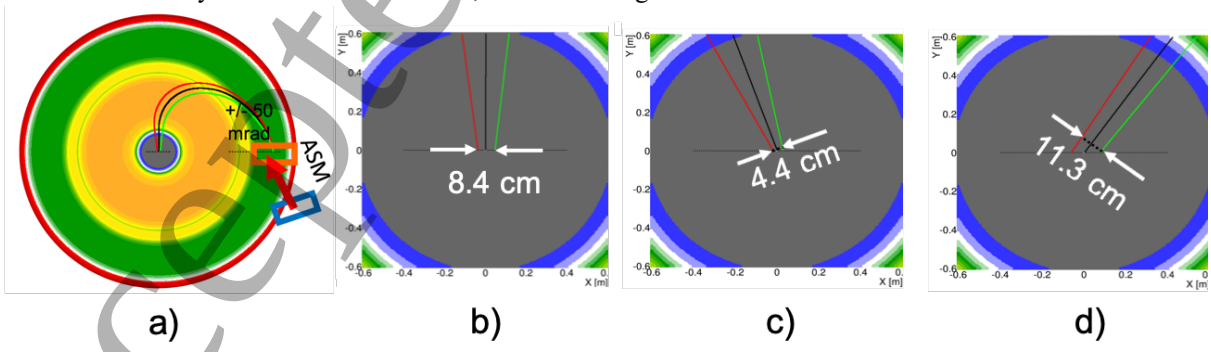

Figure 12. a) OPAL simulation of pencil beam scanning by a +/-50 mrad variation of the scanning angle in the ASM. b, c, d) Zooms of the pencil beams at the isocenter for treatment angles at 0^0, -20^0 and $+35^0$ respectively.

As can be seen in figure 12, the relation between pencil beam position and its deflection in the ASM magnet is not linear and treatment angle dependent. However, after a calibration procedure, the PBS-control algorithm can correct for such non-linearities and dependencies.

This PBS deflection is in the same order of magnitude as the deflection angle needed to cover an arc of 180 degrees. For PBS a similar speed of several mrad/ms is needed, which is within the approximate specs of the ASM system. In the axial direction, PBS can be performed by adding a perpendicular scanning direction to the ASM system. This should deflect the beam out of the bending plane into the axial direction. The maximum deflection in the axial direction is limited by the free axial space between the coils and equipment surrounding the *Central region* and expected to be in the order of 5-10 cm. This is not enough for most clinical indications, so this option has to be combined with the possibilities given by the axially sliding patient table, which is needed anyway. It is interesting to investigate spiral arc proton therapy, similar as in the Tomo-Helical Spiral-therapy system of Accuray (Accuray 2020), which is applied in photon therapy.

Although several issues, like treatment angle dependence and pencil beam size variations, still need to be worked out in more detail, we have shown that this method to perform PBS is a feasible option in the here proposed proton arc-scanning device.

3.4 Beam energy

In order to treat at different depths in the patient, different proton energies must be used at the patient. Compared with conventional proton therapy using a limited number of fields, proton arc therapy is very likely to require fewer proton energies due the increase in the degrees-of-freedom in treatment planning. However, the exact number of proton energies will still depend on tumor volume, tumor location, clinical planning goals, etc. In traditional proton therapy gantries, different energies can easily be achieved by passive systems like a ridge filter or range shifter plates. For arc therapy a ridge filter like system is not expected to be applicable.

We have concentrated on two other methods to vary the energy. The first method is a passive system shown in figure 13, which applies range shifting just before the beam enters the patient. It consists of a mechanically adjustable pair of strong, but light (e.g. fiber glass) rings surrounding the *Central region*. Each ring has one wedge shaped side in the axial direction, pointing towards the other ring. By tilting the rings towards (or away from) each other, one obtains the necessary overlap of the wedges at the azimuthal location along the ring, where the beam goes through. This is at the treatment angle θ. The amount of ring tilting and/or axial distance between the rings, determines the amount of overlap of the wedges at the beam crossing location. This sets the amount of material crossed in the wedges and thus the required range shift. For other treatment angles the needed overlap is set by adjusting the tilt and/or axial distance between the rings. With this dual ring system the range of the beam is set at any treatment angle, with only small mechanical movements of relatively light devices in the axial direction. No rotation of any device with the beam is necessary and the mass is limited, to ensure fast motions.

Due to the large distance of approx. 40 cm to the isocenter, multiple scattering in the range shifter will increase the beam size up to a few cm at the patient. Therefore we have to consider smaller diameter rings and the use of a flexible sheet of bolus material around the patient (Both *et al* 2014). Experience with the first PBS gantry have shown, that acceptable treatment plans can be achieved also with a range shifter in front of the patient if the maximum field energy is adapted and the air gap between nozzle and patient is kept small (Pedroni *et al* 2005).

In addition to this, for superficial targets, the treatment plans could be optimized. One could select only those arcs, which use a low energy to achieve the required short ranges. It has to be investigated if, how and for which indications this could be applied. If only low energies are used, an incoming beam with lower energy could be used and the magnet strengths of the device could be reduced for that treatment. The smaller fast energy modulations can be made in addition.

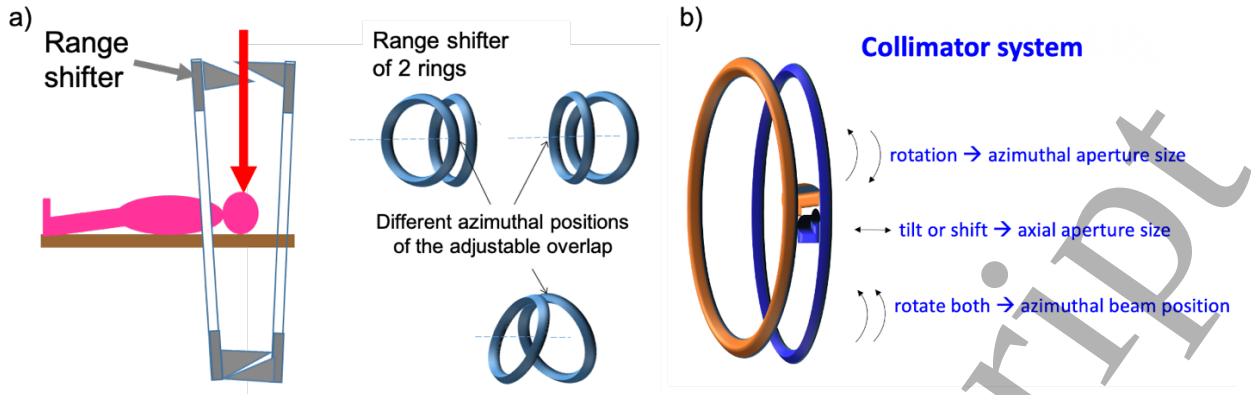

Figure 13. (a) A system of a mechanically adjustable pair of (e.g.) glass fiber rings with a graphite wedge on one side, surrounding the *Central region*. At treatment angle θ the overlap of the wedge shaped sides crossed by the beam, is determining the range. The amount of wedge-overlap and θ are set by small axial shifts and tilting of the rings.
(b) A beam collimator system to shape the beam at isocenter. The aperture between the two L-shaped blocks determines the beam size, the axial distance between the two rings determines the beam aperture in the axial direction.

The second method we investigated is an active system, in which the energy of the beam is varied in the beam transport system before entering the arc-scanning device. Due to the large inductance of the system, the magnetic fields of the *Guiding field* and the *Bending field* cannot change very quickly with beam energy. Although one could optimize the magnet design, this would limit the speed to make an energy change. Therefore, we investigated the effect of a beam energy change on the pencil beam position in the patient, when keeping the field strengths constant. Such a shift could then be compensated by the ASM system. As shown in figure 14, the effect of an energy change can be an almost parallel lateral displacement of the pencil beam in the central region. The lateral displacement corresponds to a dispersion of approximately 3.7 cm per percent of beam momentum change. Such a shift can easily be compensated by an additional lateral deflection of the pencil beam by the ASM, similar as in PBS. The accepted large momentum shifts shown in figure 14, indicate that an energy change of up to at least +/- 5% can be dealt with in this way. Also here one has to take into account that both the dispersion and the PBS compensation, will depend on the treatment angle.

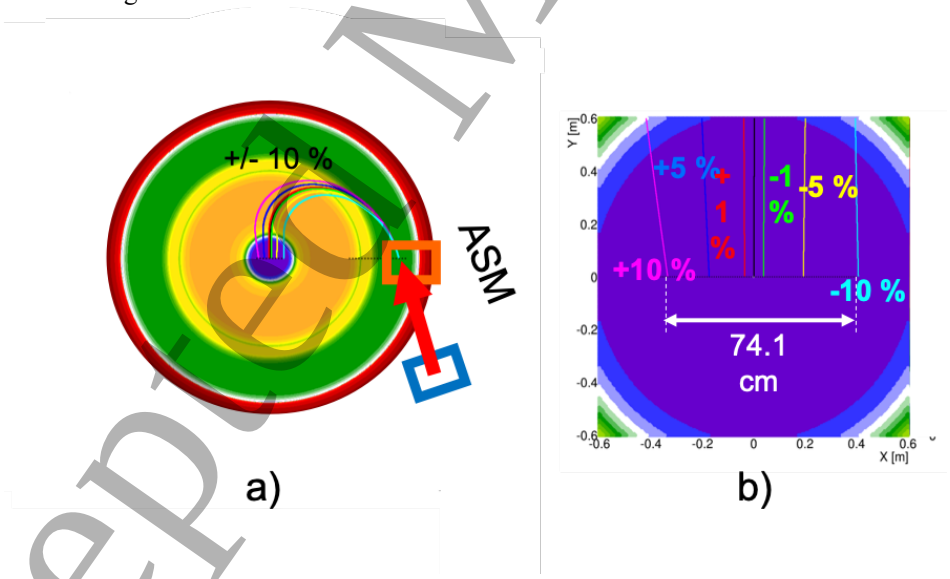

Figure 14. OPAL simulations of pencil beam shifts at the isocenter (b) due to a momentum variation (given in %dp/p) of beam.

In a next stage of the project, we also intend to investigate the application of treatment plans using mostly high energies. In such plans, only pencil beams are used that stop at the distal edge of the target. This method of DET (Distal Edge Tracking) has been proposed by Deasy *et al* (1999). If the high energies are used in combination with the use of range shifters or energy changes of the incoming beam, one could benefit from the reduced spread due to the multiple scattering (Lomax 1999). This may also be relatively easy to apply in the second method discussed above.

As mentioned above, with lateral PBS we can compensate the pencil beam shift due to an energy change. However, one has to deal with energy spread in the beam as well. In typical cyclotron driven facilities, the corresponding momentum spread in the proton beam is usually in the order of 0.5%. The observed dispersion of 3.7 cm/(%dp/p) in our system, would then give a pencil beam size of more than a cm at the patient, which is too large. Although a reduction of the momentum spread in the beam would help sufficiently, it would decrease beam intensity too much in a cyclotron driven system. Therefore we propose to install a system of a 90° bending magnet in between two quadrupole doublets to compensate the dispersion of 3.7 cm/%. As already shown in figure 2, this system will be part of the beam transport system to the arc-scanning device and will be located outside the treatment room, just before the coupling point in the ASM. Such dispersion matching methods are well known in the optics of charged particle beams (Carey 1992). For example, it is used to obtain a high resolution in magnetic spectrometers, as well as to select the right beam energy in the energy selection systems (ESS) following the degrader in a cyclotron driven proton therapy facility. Since this is a very well-known technique, we decided to make a more detailed design in a later phase.

3.5 Beam shape at isocenter

There are different possibilities to optimize the beam shape at isocenter. For future work we are considering to adjust the field modulation in the *Guiding field* region, a radial field gradient in the *Bending field* region and/or to vary the beam size at the ASM system. In case it would still be necessary to limit the beam by collimation, a dedicated collimation system has to be designed. We consider a collimation system mounted on two rings, based on the same principle as the degrader concept we show in figure 13. As presented in figure 13b, on each ring, a L-shaped block is mounted, on one ring in the normal orientation and upside-down at the opposing ring. Then the aperture between the two L-shaped blocks determines the beam size. The axial distance between the two rings determines the beam aperture in the axial direction and by rotating one ring with respect to the other, the beam aperture between blocks is varied in the azimuthal direction. The rotation of both rings has to follow the azimuthal angle of the beam. It has to be investigated at what radius the collimation has to take place, to minimize the motions in a scanning procedure.

3.6 Beam intensity

During the motion of the beam along an arc, the intensity has to be adjusted synchronously to the azimuthal beam position. Fast control of intensity variation is of advantage, so that the arc-motion is not compromised. In our study we have assumed that a 230 MeV proton beam is coming from a cyclotron system. In a cyclotron, intensity variations can be done rapidly by a beam deflection system and a collimator in the central region of the cyclotron. Such a system is in use for continuous PBS at the cyclotron of the PROSCAN system at PSI (Schippers *et al* 2008, Schätti *et al* 2014, Psoroulas *et al* 2019). The beam transmission through the collimator is regulated with an accuracy in the order of a percent by a variation of the deflection within a fraction of a millisecond.

3.7 Beam monitoring

In the here proposed arc-scanning system, a cylindrical radiation detection system has to be designed around the *Central region*, to perform high speed monitoring of the beam position, intensity and size at all treatment angles. One could think of a ring-shaped ionization chamber, consisting of several layers with different functions and associated electrode structures. Also other detector materials or systems could be considered, benefiting from the many detector developments in high-energy physics for example. It is expected that the combination of beam intensity and high speed of the dose delivery process would limit the on-line monitoring and allow only measurement results integrated over e.g. one arc sweep. This should then be verified in a dedicated QA program on dosimetry at the isocenter. However, such a system will need a thorough study of the reliability and potential risks.

4. Discussion

We have presented a novel idea of a device for fast arc-therapy with proton beams and have shown the results of a first feasibility study of this concept. This study has shown that the concept is feasible. Also, the study points out into which direction one could search for solutions for remaining open issues. More detailed investigations are needed on the consequences of

possible solutions, since solutions have to be balanced against possible negative effects on, for example, price, size, beam quality, speed, etc..

In the study presented here, we concentrate on the beam transport and beam delivery aspects and did not present a magnet design. We have used a simple model of an iron yoke based magnet to obtain a more or less realistically shaped magnetic field map. A study on the major magnet specifications, such as coil dimensions, iron, superconducting (with or without liquid helium) or normal conducting coils, forces, etc., is a major task in a follow up project. A superconducting version would enable an approximate reduction of size by a factor of 2 in radius and reduction of a factor of 4 in weight.

The goal of a new design is to achieve a field map as we have assumed in the study presented here. An extensive iterative design process is needed to deal with the inevitable deviations from the original magnetic field and the verifications by tracking calculations. In our study we have used the 3D magnetic field map derived from the iron magnet model, to perform tracking calculations. For calculations of the beam transport in certain specific regions in the magnetic field, we have applied models based on a series of consecutive bending magnets. This has been used to study crossing of the boundary between different field regions and for the beam transport in periodically varying fields in the *Guiding field* region. In this model, field configurations could be adjusted easily and enabled us to simulate possible improvements of the beam focusing along the trajectory towards the treatment isocenter. Of course, these modifications have to be included in the final specifications of the magnet. We have shown that, with these optimizations there are also other interesting possibilities for improvements. For example, an increase of the ripple amplitude in the radial field profile at the *Bending field* boundary could be used to compensate a more parallel field boundary crossing. This would help to minimize the needed radial extension of the *Guiding field*, i.e. the radial dimension of the whole device. Our pragmatic choice of $\alpha=70^0$ was just to test this method. Also, a sensitivity study is needed to investigate the dependence of the pencil beam characteristics at isocenter, from the starting conditions of the beam at the ASM system, such as radial position and direction, size, divergence, energy and energy spread. In this respect the possible advantages and disadvantages of having two or more ASM systems have to be investigated. All simulations presented here assumed a beam in "vacuum", so neglecting scatter in the range shifter, vacuum windows, beam monitors or air. As in any gantry design process, also these contributions to the beam size at isocenter have to be investigated.

We have shown that pencil beam scanning could also be performed as part of the beam delivery method. Although possible, the scanning recipe for the control system will be complicated due to its non-linear dependence on treatment angle and energy. The dependence on treatment angle is caused by the variation of the sensitivity of the Arc-scan system (figure 7), which has to be reduced. It has to be discussed where these and other corrections are taken into account in the complex process "treatment planning – steering file in control system".

Further investigations have to be performed on the energy dependence of the beam transport in the arc-scanning device and how this may be compensated. First results suggest, that an energy-shift induced displacement of the pencil beam, can be compensated by a shift in the lateral position, using the ASM system as in PBS. However, also here a significant dependence on treatment angle is expected, which has to be taken into account in the treatment planning process mentioned before. An option to be investigated is the addition of some steering coils in the *Guiding field* at azimuthal angles, at which the ASM does not have a strong variation in its pencil beam deflection.

A very interesting topic for further investigation with medical physics experts, is the possibility to shorten the treatment time. The very fast arc-scanning may enable a non-traditional order or sequence in which the different dose application processes (arcs, PBS, energy shifts, intensity variations) are applied. One could for example, apply an arc many times, but each time with a different energy and intensity profile and /or a different lateral PB scan position. A single energy per scan can benefit from a simple change in axial distance between the degrader rings, or by changing the incoming energy by up to approximately 5% and use a correction of the ASM settings to deal with the beam shift (figure 14). Such a novel sequence of beam delivery actions is to be optimized and could lead to the use of new sequences of dose application actions in this device.

One could apply the fast beam intensity regulation also to switch the beam on or off. Beam configurations that do not need to be applied, can then be ignored by switching off the beam at the appropriate moments within an arc. A fixed energy and/or PB position will need a dedicated intensity profile for each arc applied. This will need intensive simulations, which must include the timing aspect to minimize treatment time.

Treatment planning studies will be part of next studies. These will be necessary to investigate dose delivery using a reduced amount of steps (PBS positions, energies) in the delivery process (van de Water *et al* 2015 and Gu *et al* 2020). In such studies, one should then also investigate whether a reduction of the amount of steps in processes, such as setting of treatment angle, changing energy, positioning the pencil beam and varying the intensity within an arc, could be obtained by the combination of arc scanning with a novel order of dose delivery actions.

A significant reduction of used energies and, thus, a reduction of treatment time can be achieved with a technique called PMAT (Proton Monoenergetic Arc Therapy) proposed by Bertolet and Carabe (2020). This method assumes the use of monoenergetic partial arcs to enhance the dose-averaged linear energy transfer (LETd) distribution in the target leading to an

increase of the relative biological effectiveness (RBE) within the target volume. As only a few energy changes are required for each axial plane, and partial arcs could be delivered very fast without mechanical motions, our static device is a perfect candidate for future implementation of PMAT to deliver high-quality plans in a short time. In all the clinical brain cases presented by Bertolet and Carabe (2020), there are monoenergetic partial arcs as long as at least 50 degrees, and the total number of energies per axial plane is between 8 and 11. Moreover, the plans can be further optimized to find a compromise between the treatment time and plan quality. This example indicates, that in the current design phase, only qualitative predictions on a possible time reduction with the device proposed here, can be made. Like the PMAT concept, other methods of beam delivery may be possible.

To monitor the patient position and eventual motions, an X-ray device could be mounted on the patient table, similar as the Medphoton system (Medphoton 2020).

In several irradiation treatments it can be of benefit to irradiate from a non-coplanar direction. Normally this is realized by a table rotation in the horizontal plane. However, the aperture and axial extension of the arc-scanning device are limiting this tilt to a few degrees only. Increase of the aperture would have negative consequences for the pencil beam properties, due to an increased effect of scattering in the dosimetry devices and range shifter. However, a tapering of the entrance and exit of the cylindrical aperture, would allow a rotation of approximately 20^0. This would already be sufficient for e.g. treatments of non-brain tumors (Snider *et al* 2018), tumors along the spinal cord (Seravalli E *et al* 2018), complex treatments in head and neck (Frank *et al* 2014, Bizzochi *et al* 2020) and treatments of centrally located skull base tumors (Kountouri *et al* 2019). In the design of the magnet and eventual cryostat, one should take such tapering into account.

With respect to the layout or configuration of the system, it should be noted, that the *Central region* need not be field free in principle. It was just a choice we made, to make the conceptual simulations easier. In general, a field free region is often required to allow certain clinical equipment and pacemakers near the treatment region. But one could investigate if it makes sense to combine the proton arc-scan device with an MRI functionality just before or during the dose application.

5. Conclusions

We can conclude that a first study of our conceptual ideas and some initial designs have shown possibilities of the here presented fast proton arc-scanning system. These may enable a new way of thinking on how the dose delivery can be performed, such as for example by applying new ways of angular variability in treatments. Shorter treatment times could be achieved by the ideas presented in this technical concept:

- no mechanical rotation of a heavy components,
- arc scanning by adjustment of a set of small scanning magnets,
- a dual ring system for range shifting of the PBS,
- compensation of the PBS-shift due to energy variation, by correcting the arc-scanning magnets.

A quantitative estimate of the treatment time reduction is only possible after certain choices have been made and further studies have been done. These issues also indicate the most important remaining open challenges in our proposal. In the next steps of the design process, these have to be dealt with and different treatment methods have to be simulated and evaluated to make such choices. This will then provide the starting points to prepare a prototype production.

Acknowledgements

We kindly acknowledge Prof. Dr. med. Damien C. Weber from the Center for Proton Therapy at the Paul Scherrer Institute for his support on the clinical aspects in this paper.

References

Accuray 2020 Website of Accuray: www.accuray.com/tomotherapy

Adelmann A et al 2008–2018 The OPAL (Object Oriented Parallel Accelerator Library) framework *Technical Report* PSI-PR-08-02, Paul Scherrer Institute

Berz M 1990 Computational aspects of optics design and simulation: COSY INFINITY *Nucl. Instrum. Methods Phys. Res.* A 298 473-9

Bertolet A and Carabe A 2020 Proton monoenergetic arc therapy (PMAT) to enhance LETd within the target *Phys. Med. Biol.* 65 0–11

Bizzocchi N, Albertini F, Böhlen T T, Bachtiary B, Bolsi A, Rosas S, Lomax A J, Weber D C, Hrbacek J 2020 Pencil beam scanning proton therapy planning using a split target paradigm for bilateral lymph node irradiation in head and neck cancer *In preparation*

Both S *et al* 2014 Development and clinical implementation of a universal bolus to maintain spot size during delivery of base of skull pencil beam scanning proton therapy *Int. J. Rad. Onc. Biol. Phys.* 90(1):79-84

Carey D C 1992, *The Optics of Charged Particle beams, section 5.6*, (Horwood Acad.Publ.)

Chiavassa S, Bessieres I, Edouard M, Mathot M, Moignier A 2019 Complexity metrics for IMRT and VMAT plans: a review of current literature and applications *Br. J. Radiol.* 92(1102):20190270

Craddock M K 2009 AG focusing in the Thomas cyclotron of 1938 (*Proc. Particle Accelerator Conf. PAC09*) pp 5041-5043

Deasy J O, Shephard D M and Mackie T R 1997 Distal edge tracking: a proposed delivery method for conformal proton therapy using intensity modulation *Proc. 12th ICCR (Salt Lake City) ed D D Leavitt and G S Starkschall (Madison, WI: Medical Physics Publishing)* pp 406–9

Ding X *et al* 2016 Spot-Scanning Proton Arc (SPArc) Therapy – The first robust and delivery-efficient spot-scanning arc therapy *Int. J. Rad. Onc. Biol. Phys.* 96(5):1107-1116.

Ernult 2018 https://iba-worldwide.com/content/iba-and-beaumont-hospital-s-cancer-institute-royal-oak-michigan-announce-first-irradiation

Frank S J, Cox J D, Gillin M, Mohan R, Garden A S, Rosenthal D I *et al* 2014 Multifield Optimization Intensity Modulated Proton Therapy for Head and Neck Tumors: A Translation to Practice *Int. J. Radiat. Oncol. Biol. Phys.* 89(4):846-53

Gu W, Ruan D, Lyu Q, Zou W, Dong L, Sheng K 2020 A novel energy layer optimization framework for spot-scanning proton arc therapy Med. Phys. 47(5): 2072-2084

Kountouri M, Pica A, Walser M, Albertini F, Bolsi A, Kliebsch U *et al* 2019 Radiation-induced optic neuropathy after pencil beam scanning proton therapy for skull-base and head and neck tumours *Br. J. Radiol.* 93(1107):20190028

Li X *et al* 2019 The first prototype of spot-scanning proton arc treatment delivery, *Radiother Oncol.* 137:130-136

Lomax 1999 Intensity modulation methods for proton radiotherapy Phys. Med. Biol. 44 185-205

Matlab 2020 Website of Mathworks: mathworks.com/de/products/matlab.html

Medphoton 2020 Website of MedPhoton GmbH: www.medphoton.at

Menzel M T and Stokes H K 1987 User's Guide for POISSON / SUPERFISH group of codes *Technical Report* LA-UR-87-115 DOI:10.2172/10140823, Los Alamos National Lab

Meot F 2012 Zgoubi Users' Guide http://www.bnl.gov/isd/documents/79375.pdf *Report* BNL-98726-2012-IR), Brookhaven National Laboratory

Nicolini G, Clivio A, Cozzi L, Fogliata A, Vanetti E 2011 On the impact of dose rate variation upon RapidArc implementation of volumetric modulated arc therapy *Med. Phys.* 38: 264–71

Pedroni E, Scheib S, Böhringer T, Coray A, Grossmann M, Lin S, and Lomax A 2005 Experimental characterization and physical modelling of the dose distribution of scanned proton pencil beams *Phys. Med. Biol. 50 541-561*

Psoroulas S, Fernandez Carmona P, Meer D, Weber D C 2019 On-line dynamic beam intensity control in a proton therapy cyclotron In (*Proc. 20th Int. Conf. on Cyclotrons*) TUB04

Sandison G A *et al* 1997 Phantom assessment of lung dose from proton arc therapy *Int. J. Oncol. Phys*. 38: 891-897

Schätti A, Meer D, Lomax A J 2014 First experimental results of motion mitigation by continuous line scanning of protons *Phys. Med. Biol.* 59 5707

Schulze M E 1991 Commissioning Results of the LLUMC Beam Switchyard and Gantry, (*Proc. 14th Particle Accelerator Conf. PAC'91*), pp 610-613

Schippers J M *et al* 2008 First year of operation of PSI's new SC cyclotron and beam lines for proton therapy (*Proc. 18th Int. Conf. on Cyclotron Appl. 2007*) pp15-17

Seravalli E, Bosman M, Lassen-Ramshad Y, Vestergaard A, Oldenburger F, Visser J *et al* 2018 Dosimetric comparison of five different techniques for craniospinal irradiation across 15 European centers: analysis on behalf of the SIOP-E-BTG (radiotherapy working group) *Acta Oncol.* 57(9):1240-49

Snider J W, Schneider R A, Poelma-Tap D, Stieb S, Murray F R, Placidi L *et al* 2018 Long-Term Outcomes and Prognostic Factors After Pencil-Beam Scanning Proton Radiation Therapy for Spinal Chordomas: A Large, Single-Institution Cohort *Int. J. Radiat. Oncol. Biol. Phys.* 101(1):226-33

Teoh M, Clark C H, Wood K, Whitaker S, Nisbet A 2011 Volumetric modulated arc therapy: a review of current literature and clinical use in practice, *Br. J. Radiol.* 84(1007):967-96

van de Water S, Kooy H M, Heijmen B J M and Hoogeman M S 2015 Shortening Delivery Times of Intensity Modulated Proton Therapy by Reducing Proton Energy Layers During Treatment Plan Optimization *Int. J. Radiat. Oncol. Biol. Phys.* 92 460–8